Difference-frequency generation of optical radiation from two-color x-ray pulses

E. Shwartz[1,*] and S. Shwartz[2]

[1]*The Physics Department, Bar Ilan University, Ramat Gan 5290002, Israel*
[2]*The Institute for Nanotechnology and Advanced Materials, Bar Ilan University, Ramat Gan 5290002, Israel*
[*]*eli.shwartz@gmail.com*

Abstract: We describe the process of difference-frequency generation of short optical pulses from two-color X-ray pulses. By assuming 10^{11} photons per X-ray pulse, we predict that the optical count rate can exceed 10^{7} photons per pulse. Similar to other effects involving nonlinear interactions of X-rays and optical radiation, the effect we describe can be used for microscopic studies of chemical bonds and as a probe for light-matter interactions on the atomic scale. Since the X-ray damage threshold is much higher than the optical damage threshold, the efficiency of difference-frequency generation from two X-ray pulses is expected to be orders of magnitude higher than the efficiency of effects such as sum/difference-frequency mixing between X-rays and optical intense short-pulse sources.

OCIS codes: (190.4180) Multiphoton processes; (190.4223) Nonlinear wave mixing; (340.7480) X-rays, soft x-rays, extreme ultraviolet (EUV); (320.5390) Picosecond phenomena; (320.5550) Pulses.

References and links

1. I. Freund and B. F. Levine, "Optically modulated X-ray diffraction," Phys. Rev. Lett. **25**(18), 1241–1245 (1970).
2. P. M. Eisenberger and S. L. McCall, "Mixing of X-ray and optical photons," Phys. Rev. A **3**(3), 1145–1151 (1971).
3. T. E. Glover, D. M. Fritz, M. Cammarata, T. K. Allison, S. Coh, J. M. Feldkamp, H. Lemke, D. Zhu, Y. Feng, R. N. Coffee, M. Fuchs, S. Ghimire, J. Chen, S. Shwartz, D. A. Reis, S. E. Harris, and J. B. Hastings, "X-ray and optical wave mixing," Nature **488**(7413), 603–608 (2012).
4. P. L. Shkolnikov and A. E. Kaplan, "X-ray third-harmonic generation in plasmas of alkalilike ions," Opt. Lett. **16**(24), 1973–1975 (1991).
5. P. L. Shkolnikov and A. E. Kaplan, "Feasibility of x-ray resonant nonlinear effects in plasmas," Opt. Lett. **16**(15), 1153–1155 (1991).
6. C. Conti, A. Fratalocchi, G. Ruocco, and F. Sette, "Nonlinear optics in the X-ray regime: nonlinear waves and self-action effects," Opt. Express **16**(12), 8324–8331 (2008).
7. A. Nazarkin, S. Podorov, I. Uschmann, E. Förster, and R. Sauerbrey, "Nonlinear optics in the angstrom regime: hard-X-ray frequency doubling in perfect crystals," Phys. Rev. A **67**(4), 041804 (2003).
8. U. Harbola and S. Mukamel, "Coherent stimulated X-ray Raman spectroscopy: attosecond extension of resonant inelastic X-ray Raman scattering," Phys. Rev. B **79**(8), 085108 (2009).
9. P. Eisenberger and S. L. McCall, "X-ray parametric conversion," Phys. Rev. Lett. **26**(12), 684–688 (1971).
10. B. Adams, P. Fernandez, W. K. Lee, G. Materlik, D. M. Mills, and D. V. Novikov, "Parametric down conversion of X-ray photons," J. Synchrotron Radiat. **7**(Pt 2), 81–88 (2000).
11. S. Shwartz, R. N. Coffee, J. M. Feldkamp, Y. Feng, J. B. Hastings, G. Y. Yin, and S. E. Harris, "X-ray parametric down-conversion in the Langevin regime," Phys. Rev. Lett. **109**(1), 013602 (2012).
12. G. Doumy, C. Roedig, S. K. Son, C. I. Blaga, A. D. DiChiara, R. Santra, N. Berrah, C. Bostedt, J. D. Bozek, P. H. Bucksbaum, J. P. Cryan, L. Fang, S. Ghimire, J. M. Glownia, M. Hoener, E. P. Kanter, B. Krässig, M. Kuebel, M. Messerschmidt, G. G. Paulus, D. A. Reis, N. Rohringer, L. Young, P. Agostini, and L. F. DiMauro, "Nonlinear atomic response to intense ultrashort X rays," Phys. Rev. Lett. **106**(8), 083002 (2011).
13. K. Tamasaku, E. Shigemasa, Y. Inubushi, T. Katayama, K. Sawada, H. Yumoto, H. Ohashi, H. Mimura, M. Yabashi, K. Yamauchi, and T. Ishikawa, "X-ray two-photon absorption competing against single and sequential multiphoton processes," Nat. Photonics **8**(4), 313–316 (2014).
14. C. Weninger, M. Purvis, D. Ryan, R. A. London, J. D. Bozek, C. Bostedt, A. Graf, G. Brown, J. J. Rocca, and N. Rohringer, "Stimulated electronic X-ray Raman scattering," Phys. Rev. Lett. **111**(23), 233902 (2013).
15. S. Shwartz, M. Fuchs, J. B. Hastings, Y. Inubushi, T. Ishikawa, T. Katayama, D. A. Reis, T. Sato, K. Tono, M. Yabashi, S. Yudovich, and S. E. Harris, "X-ray second harmonic generation," Phys. Rev. Lett. **112**(16), 163901 (2014).

#226995 - $15.00 USD Received 17 Nov 2014; revised 10 Feb 2015; accepted 12 Feb 2015; published 13 Mar 2015

16. H. Danino and I. Freund, "Parametric down conversion of X rays into the extreme ultraviolet," Phys. Rev. Lett. **46**(17), 1127–1130 (1981).
17. K. Tamasaku and T. Ishikawa, "Idler energy dependence of nonlinear diffraction in XX + EUV parametric down-conversion," Acta Crystallogr. A **63**(Pt 5), 437–438 (2007).
18. K. Tamasaku and T. Ishikawa, "Interference between Compton scattering and X-ray parametric down-conversion," Phys. Rev. Lett. **98**(24), 244801 (2007).
19. K. Tamasaku, K. Sawada, E. Nishibori, and T. Ishikawa, "Visualizing the local optical response to extreme-ultraviolet radiation with a resolution of λ/380," Nat. Phys. **7**(9), 705–708 (2011).
20. P. Emma, R. Akre, J. Arthur, R. Bionta, C. Bostedt, J. Bozek, A. Brachmann, P. Bucksbaum, R. Coffee, F. J. Decker, Y. Ding, D. Dowell, S. Edstrom, A. Fisher, J. Frisch, S. Gilevich, J. Hastings, G. Hays, P. Hering, Z. Huang, R. Iverson, H. Loos, M. Messerschmidt, A. Miahnahri, S. Moeller, H. D. Nuhn, G. Pile, D. Ratner, J. Rzepiela, D. Schultz, T. Smith, P. Stefan, H. Tompkins, J. Turner, J. Welch, W. White, J. Wu, G. Yocky, and J. Galayda, "First lasing and operation of an ångstrom-wavelength free-electron laser," Nat. Photonics **4**(9), 641–647 (2010).
21. B. W. McNeil and N. R. Thompson, "X-ray free-electron lasers," Nat. Photonics **4**(12), 814–821 (2010).
22. T. Hara, Y. Inubushi, T. Katayama, T. Sato, H. Tanaka, T. Tanaka, T. Togashi, K. Togawa, K. Tono, M. Yabashi, and T. Ishikawa, "Two-colour hard X-ray free-electron laser with wide tunability," Nat Commun **4**, 2919 (2013).
23. A. A. Lutman, R. Coffee, Y. Ding, Z. Huang, J. Krzywinski, T. Maxwell, M. Messerschmidt, and H. D. Nuhn, "Experimental demonstration of femtosecond two-color X-ray free-electron lasers," Phys. Rev. Lett. **110**(13), 134801 (2013).
24. A. A. Lutman, F. J. Decker, J. Arthur, M. Chollet, Y. Feng, J. Hastings, Z. Huang, H. Lemke, H. D. Nuhn, A. Marinelli, J. L. Turner, S. Wakatsuki, J. Welch, and D. Zhu, "Demonstration of single-crystal self-seeded two-color X-ray free-electron lasers," Phys. Rev. Lett. **113**(25), 254801 (2014).
25. Y. R. Shen, *The Principles of Nonlinear Optics* (Wiley-Interscience, 2003), Chap. 1.
26. R. W. Boyd, *Nonlinear Optics* (Academic, 2003), Chap. 3.
27. All the simplifications we used allow us to present a simple and very clear result for the signal field, however this is not essential for the solution of Eq. (3).
28. E. Allaria, R. Appio, L. Badano, W. A. Barletta, S. Bassanese, S. G. Biedron, A. Borga, E. Busetto, D. Castronovo, P. Cinquegrana, S. Cleva, D. Cocco, M. Cornacchia, P. Craievich, I. Cudin, G. D'Auria, M. Dal Forno, M. B. Danailov, R. De Monte, G. De Ninno, P. Delgiusto, A. Demidovich, S. Di Mitri, B. Diviacco, A. Fabris, R. Fabris, W. Fawley, M. Ferianis, E. Ferrari, S. Ferry, L. Froehlich, P. Furlan, G. Gaio, F. Gelmetti, L. Giannessi, M. Giannini, R. Gobessi, R. Ivanov, E. Karantzoulis, M. Lonza, A. Lutman, B. Mahieu, M. Milloch, S. V. Milton, M. Musardo, I. Nikolov, S. Noe, F. Parmigiani, G. Penco, M. Petronio, L. Pivetta, M. Predonzani, F. Rossi, L. Rumiz, A. Salom, C. Scafuri, C. Serpico, P. Sigalotti, S. Spampinati, C. Spezzani, M. Svandrlik, C. Svetina, S. Tazzari, M. Trovo, R. Umer, A. Vascotto, M. Veronese, R. Visintini, M. Zaccaria, D. Zangrando, and M. Zangrando, "Highly coherent and stable pulses from the FERMI seeded free-electron laser in the extreme ultraviolet," Nat. Photonics **6**(10), 699–704 (2012).
29. C. Bostedt, J. D. Bozek, P. H. Bucksbaum, R. N. Coffee, J. B. Hastings, Z. Huang, R. W. Lee, S. Schorb, J. N. Corlett, P. Denes, P. Emma, R. W. Falcone, R. W. Schoenlein, G. Doumy, E. P. Kanter, B. Kraessig, S. Southworth, L. Young, L. Fang, M. Hoener, N. Berrah, C. Roedig, and L. F. DiMauro, "Ultra-fast and ultra-intense X-ray sciences: first results from the LINAC coherent light source free-electron laser," J. Phys. At. Mol. Opt. Phys. **46**(16), 164003 (2013).
30. D. J. Dunning, B. W. J. McNeil, and N. R. Thompson, "Towards zeptosecond-scale pulses from X-ray free-electron lasers," arXiv preprint arXiv:1309.0444 (2013).
31. J. R. Lakowicz, *Principles of Fluorescence Spectroscopy* (Springer, 2006).
32. A. M. Zaitsev, *Optical Properties of Diamond: a Data Handbook* (Springer, 2001), Chap. 8.
33. J. R. Fienup, "Phase retrieval algorithms: a comparison," Appl. Opt. **21**(15), 2758–2769 (1982).

1. Introduction

About forty years ago Freund & Levine [1] and Eisenberger & McCall [2] described the nonlinear interactions between X-rays and optical radiation. Those studies addressed several nonlinear processes including parametric down conversion (PDC) of X-rays into the optical region [1], sum-frequency generation (SFG) and difference-frequency generation (DFG) of X-rays and optical pulses [1–3]. In the process of PDC of X-rays into visible light, a pump at X-ray wavelengths interacts with the vacuum field to generate two beams, one at X-ray wavelengths and the other at optical wavelengths. In the processes of SFG and DFG an intense optical beam interacts with an X-ray beam to generate a frequency-shifted X-ray beam. The authors of those papers highlighted the possibility of using the nonlinear interactions between X-rays and optical radiation as a probe to study the microscopic structure of chemical bonds and the density of valence electrons including the response to optical radiation with the atomic-scale resolution. However, until very recently there were no experimental evidence for nonlinear interactions between X-rays and optical radiation due to

#226995 - $15.00 USD Received 17 Nov 2014; revised 10 Feb 2015; accepted 12 Feb 2015; published 13 Mar 2015

absence of sufficiently bright X-ray sources. The new X-ray free-electron lasers enabled the observation of X-ray and optical frequency mixing. In a recent work, an X-ray beam at 8 keV (1.5498 Å) interacted with an intense optical beam at 1.5 eV (800 nm) to generate an X-ray beam at 8.0015 keV (1.5495 Å) [3]. The efficiency of the SFG process reported in that experiment was limited by the optical damage threshold and was estimated to be 3×10^{-7}. We note several pertinent effects. Three-wave-mixing [4], self-action effects [5,6], two-wave-mixing [7], and stimulated Raman scattering [8] at X-ray wavelengths have been analyzed. Experimental observations of PDC [9–11], Two-photon absorption [12,13], X-ray stimulated Raman scattering [14], and second harmonic generation [15] have been reported. Another pertinent effect is PDC of X-rays into the extreme ultraviolet (UV) regime [16–19]. In this type of nonlinear effects, the ultraviolet light is absorbed and only the hard X-ray wave is detected. Recently, it was shown experimentally that the response of the material to the UV radiation can be extracted from the measurement of the X-ray photons [19].

Here we explore the possibility of observing DFG of optical radiation from X-ray pulses [20,21]. In particular, we consider the generation of short optical pulses (typically a few hundred femtoseconds) from two transform-limited X-ray pulses at different central wavelengths. We show that with pump intensity of 10^{11} photons per pulse the generated optical signal is expected to exceed 10^7 photons per pulse, which is much higher than the expected background signals. We find that the frequency bandwidth and angular distribution of the generated signal are narrow.

The typical damage threshold of various materials at hard X-ray wavelengths is many orders of magnitude larger than the optical damage threshold. Consequently, the efficiency of DFG effect we describe here is expected to be orders of magnitude larger than the efficiency of an X-ray and optical mixing process, where one of the pumping beams is in the optical range.

Two X-ray pulses with different central frequencies are generated by propagating a single stream of relativistic bunched electrons and a seeded pulse through two slightly different undulators [22–24]. The delay between the pulses is controlled by delaying the electron stream using a magnetic chicane to overlap spatially with the narrow-bandwidth tail of the X-ray pulse in the second undulator section. We note that the two-color X-ray pulses are jitter free [22]. On the other hand, the jitter between X-ray pulses emerging form the XFEL and visible pulses emerging from the interacting optical laser is significant leading to larger experimental errors and lower efficiencies [3].

2. Model

2.1 Nonlinear wave equation

We consider a nonlinear three-wave-mixing process where two intense X-ray pulses at central photon-energies far above any electronic resonances generate an optical pulse at a central photon-energy far below the band-gap of a nonlinear crystal. We therefore consider a classical model for DFG, where the generation and the propagation of the optical radiation are described by the Maxwell's equations and where the wave-mixing process is introduced by the classical nonlinear current density. We note that the efficiency of SFG predicted by this model is with a good agreement with the results of the recent experiment by Glover *et al*. [3]. The wave equation of the generated optical field is

$$\vec{\nabla}^2\vec{\mathcal{E}} - \frac{1}{c^2}\frac{\partial^2\vec{\mathcal{E}}}{\partial t^2} = \mu_0\left(\frac{\partial^2\vec{\mathcal{P}}}{\partial t^2} + \frac{\partial\vec{\mathcal{J}}}{\partial t}\right) \tag{1}$$

where $\vec{\mathcal{E}}(\vec{r},t)$ is the electric field of the generated optical wave, c is the speed of light in vacuum, μ_0 is the vacuum permeability, $\vec{\mathcal{P}}(\vec{r},t)$ is the linear polarization, and $\vec{\mathcal{J}}(\vec{r},t)$ is the nonlinear current density, where $\vec{r} = x\hat{x} + y\hat{y} + z\hat{z}$.

#226995 - $15.00 USD Received 17 Nov 2014; revised 10 Feb 2015; accepted 12 Feb 2015; published 13 Mar 2015

As described in Fig. 1, we consider a semi-infinite slab geometry and denote *x* and *y* as the coordinates parallel to the surface, and *z* as the coordinate normal to the surface. We assume that the wave-vectors of the pump and the optical beams are in the *x*-*z* plane and that all the fields are linearly polarized in the $\hat{y}$ direction. We Fourier transform all pertinent quantities with respect to time and the coordinates parallel to the surface of the slab. For example, the Fourier transform of the electric field is $\vec{\mathbf{E}}(k_x,k_y,z,\Omega)=(2\pi)^{-3}\int_{-\infty}^{\infty}\int_{-\infty}^{\infty}\int_{-\infty}^{\infty}\vec{\mathcal{E}}(z,x,y,t)\exp(ik_x x+ik_y y-i\Omega t)dxdydt$. We introduce the linear polarization $\vec{\mathbf{P}}(k_x,k_y,z,\Omega)=\epsilon_0(n^2-1)\vec{\mathbf{E}}(k_x,k_y,z,\Omega)$ into the transformed equation, where *n* is the refractive index at the optical frequency and ϵ_0 is the vacuum permittivity. The values for *n* are retrieved using the Sellmeier equation, and the values for the X-ray refractive index were retrieved from tabulated data. We obtain,

$$\frac{\partial^2\vec{\mathbf{E}}}{\partial z^2}+k_z^2\vec{\mathbf{E}}=-i\mu_0\Omega\vec{\mathbf{J}}(z,k_x,k_y,\Omega) \tag{2}$$

where $\vec{\mathbf{J}}$ is the Fourier transform of the nonlinear current density with respect to time and the coordinates parallel to the slab, $k=n\Omega/c$, and $k^2=k_x^2+k_y^2+k_z^2$. We note that Eq. (2) is accurate and contains dispersion and diffraction to all orders.

2.2 Slowly varying envelope equation

While Eq. (2) is solvable (analytically in some cases) for a given current density, we consider an optical electric field of the form $\vec{\mathbf{E}}(k_x,k_y,z,\Omega)=\frac{1}{2}E(k_x,k_y,z,\Omega)\exp(ik_z z)\hat{y}+c.c.$ where *E* is an envelope that varies slowly as compared to the optical wave-number in the z-direction. The approximation $|2ik_z\partial_z E|>>|\partial_z^2 E|$ is adequate for the description of DFG from X-ray to the optical regime, when the temporal and spatial widths of the driving X-ray pulses are much larger than a single optical-cycle and the center wavelength, respectively. The slowly varying envelope equation is:

$$\frac{\partial E}{\partial z}=-\frac{\mu_0\Omega}{k_z}\vec{\mathbf{J}}\exp(-ik_z z)\cdot\hat{y} \tag{3}$$

We note Eq. (3) is correct for every nonlinear current density, as long as the optical field satisfies the slowly varying envelope approximation.

2.3 Nonlinear current density

The expression for the DFG nonlinear current density corresponds to the second order series expansion of the current density

$$\vec{\mathcal{J}}_\Omega^{(2)}(\vec{r},t)=\rho_0(\vec{r})\vec{v}_\Omega^{(2)}(\vec{r},t)+\rho_{\omega_1}^{(1)}(\vec{r})\vec{v}_{\omega_2}^{(1)*}(\vec{r},t)+\rho_{\omega_2}^{(1)*}(\vec{r})\vec{v}_{\omega_1}^{(1)}(\vec{r},t) \tag{4}$$

where $\rho_0=\frac{1}{2}\Sigma_m\rho_m\exp(i\vec{G}_m\cdot\vec{r})+c.c.$ is the electron density in the absence of the X-ray fields. ρ_G is the Fourier component corresponding to the reciprocal lattice vector G. $\vec{\mathbf{v}}_{\omega_1}^{(1)}$, $\vec{\mathbf{v}}_{\omega_2}^{(1)}$, $\rho_{\omega_1}^{(1)}$ and $\rho_{\omega_2}^{(1)}$ are the electron velocities and the electron densities oscillating at frequencies ω_1 and ω_2, respectively and $\vec{\mathbf{v}}_\Omega^{(2)}$ is the electron velocity that corresponds to the DFG process, with $\Omega=\omega_1-\omega_2$.

For the calculation of the nonlinear current density, we consider a DFG process where all pertinent photon-energies are far from the electronic resonance, and use a classical model

#226995 - $15.00 USD Received 17 Nov 2014; revised 10 Feb 2015; accepted 12 Feb 2015; published 13 Mar 2015

based on the Lorentz equation of motion and the continuity equation for the calculation of the electron velocities and charge densities.

$$\frac{\partial \vec{v}}{\partial t} + (\vec{v}\cdot\vec{\nabla})\vec{v} + \omega_0^2 \vec{r} = \frac{q}{m}(\vec{\mathcal{E}}^{(p)} + \vec{v}\times\vec{\mathcal{B}}^{(p)}) \tag{5}$$

$$\frac{\partial \rho}{\partial t} + \vec{\nabla}\cdot(\rho\vec{v}) = 0 \tag{6}$$

here v, r, q, m are the electron velocity, deviation from the equilibrium position, charge and mass, $\vec{\mathcal{E}}^{(p)}$ and $\vec{\mathcal{B}}^{(p)}$ are the electric and magnetic fields of the pumping beams, c is the speed of light in vacuum and ω_0 is the resonance frequency of the valence electrons. Since the magnitude of the electric force is much larger than Lorentz force, the equations can be solved by using a perturbation approach, similar to the calculations of the nonlinear current density in plasma [3,25]. We expand the quantities in Eq. (5) and (6) in power series. For example, the velocity is written as $v = v^{(1)} + v^{(2)} + \ldots + v^{(n)}$. We assume that each of the pump waves can be written as a product of a slowly varying envelope and a carrier wave, so the pump fields are $\vec{\mathcal{E}}_{1,2}^{(p)}(\vec{r},t) = \frac{1}{2}E_{1,2}^{(p)}(\vec{r},t)\exp(i\vec{k}_{1,2}\cdot\vec{r} - i\omega_{1,2}t)\hat{y} + c.c.$, where $k_{1,2}$ are the central wave-vectors. We assume a transform limited Gaussian envelope, so each of the pump fields is written as

$$E_{1,2}^{(p)}(\vec{r},t) = \left(\frac{2}{\pi}\right)^{3/4}\sqrt{\frac{\sqrt{N}\,|\cos\theta_{1,2}|}{w_{y(1,2)}w_{x(1,2)}\tau}}\exp\left[-\left(\frac{t_{1,2}+\Delta\tau_1+z'_{1,2}/v_g}{\tau_{1,2}}\right)^2 - \left(\frac{x'_{1,2}}{w_{x(1,2)}}\right)^2 - \left(\frac{y}{w_{y(1,2)}}\right)^2\right] \tag{7}$$

Here N is the number of photons per pulse, w_x and w_y are the beam minimal waists in the x' and y directions, τ is the pulse duration at full width half maximum, $\Delta\tau_1$ is the delay between the first and second X-ray beam and v_g is the group velocity in the direction of propagation of each of the X-ray waves. We define $x'_{1,2} = x\cos\theta_{1,2} - z\sin\theta_{1,2}$ and $z'_{1,2} = z\cos\theta_{1,2} + x\sin\theta_{1,2}$, where θ_1 and θ_2 are the angles of the pumping beams k vectors with respect to the normal of the crystal surface (see Fig. 1).

Since ω_0 is much smaller than ω_1, ω_2, the first order equation of motion is $\partial_t^2\vec{r}^{(1)} = q\vec{\mathcal{E}}^{(p)}/m$. The solution is $\vec{v}_{1,2}^{(1)} = \frac{iq}{2m\omega_{1,2}}E_{1,2}^{(p)}\exp(i\vec{k}_{1,2}\cdot\hat{r} - i\omega_{1,2}t)\hat{y}$. Next, we substitute the first order velocities in the second order equation of motion,

$$\frac{\partial^2\vec{r}^{(2)}}{\partial t^2} + \omega_0^2\vec{r}^{(2)} + (\vec{v}_2^{(1)*}\cdot\vec{\nabla})\vec{v}_1^{(1)} + (\vec{v}_1^{(1)}\cdot\vec{\nabla})\vec{v}_2^{(1)*} = \frac{q}{m}\left(\vec{v}_1^{(1)}\times\vec{\mathcal{B}}_2^{(p)*} + \vec{v}_2^{(1)*}\times\vec{\mathcal{B}}_1^{(p)}\right) \tag{8}$$

The solution of Eq. (8) is

$$\vec{v}^{(2)} = -\frac{iq^2\Omega}{4m^2\omega_1\omega_2(\omega_0^2-\Omega^2)}\vec{\nabla}(E_1^{(p)}\cdot E_2^{(p)*})\exp[i(\vec{k}_1-\vec{k}_2)\cdot\vec{r} - i\Omega t]\hat{y} \tag{9}$$

We substitute the first order velocity in the continuity equation and solve to obtain the charge density oscillating at Ω, $\rho_{\omega_1,\omega_2} = -\frac{q}{2m\omega_{1,2}^2}E_{1,2}^{(p)}\exp(i\vec{k}_{1,2}\cdot\hat{z} - i\omega_{1,2}t)\vec{\nabla}\rho_0\cdot\hat{y}$, where we assume that there are no free charges in the medium.

Finally, we substitute the electron velocity and charge density in Eq. (4). We neglect the terms $\rho(\omega_1)v^*(\omega_2)$, $\rho^*(\omega_2)v(\omega_1)$, since they are four orders of magnitude smaller than the Lorentz term.

The envelope quantity of the nonlinear current density is

#226995 - $15.00 USD Received 17 Nov 2014; revised 10 Feb 2015; accepted 12 Feb 2015; published 13 Mar 2015

$$J(k_x, k_y, z, \Omega) = \tilde{\kappa}\mathbf{E}_1^{(p)}(k_{1x}, k_{1y}, z, \omega_1) * \mathbf{E}_2^{(p)*}(k_{2x}, k_{2y}, z, \omega_2) \quad (10)$$

where $\mathbf{E}_1^{(p)}$ and $\mathbf{E}_2^{(p)}$ are Fourier transform of the signal field with respect to time and the coordinates parallel to the slab, and we denote $\tilde{\kappa} = q\Omega(k_1 \sin\theta_1 - k_2 \sin\theta_2)(n^2 - 1)/4m\omega_1\omega_2$. We note that $\tilde{\kappa}$ is nearly constant over the range of frequencies we consider in our problem. As noted by the early papers [26], we apply a procedure that naturally accounts for local field effects, and the nonlinear current density in Eq. (10) can be considered as a macroscopic quantity.

2.4 Phase matching

We substitute the nonlinear current density in Eq. (3) and obtain,

$$\frac{\partial E(z)}{\partial z} = -\kappa J \exp[i(k_{1z} - k_{2z} - G_z - k_z)z] + c.c. \quad (11)$$

The maximum conversion efficiency is obtained when the k-vectors satisfy the equation $\vec{k}_1 - \vec{k}_2 = \vec{G} + \vec{k}$, which is the phase matching condition in our problem. As described in Fig. 1, we consider a phase-matching scheme where all pertinent k vectors are in the same plane, denoted as the scattering plane. When the central wave vectors of the pertinent waves satisfy the phase matching condition only the Fourier component of the electron density corresponding to the reciprocal lattice vector $\vec{G}$ contributes to the nonlinear current density.

From the phase matching condition we obtain that κ, the coefficient of the nonlinear current, is expressed as,

$$\kappa = \frac{q\Omega(n^2 - 1)}{4mc\omega_1\omega_2 n} G \sin\theta_g \quad (12)$$

The implication of Eq. (11) and (12) is that even though the wavelengths of generated field are in the optical range, the strength of the field (and therefore the power) is proportional to the Fourier component of the electron charge density corresponding to the selected reciprocal lattice vector. This quantity is on the order on the atomic scale, thus the DFG process can be used as a probe for atomic-scale periodic structures.

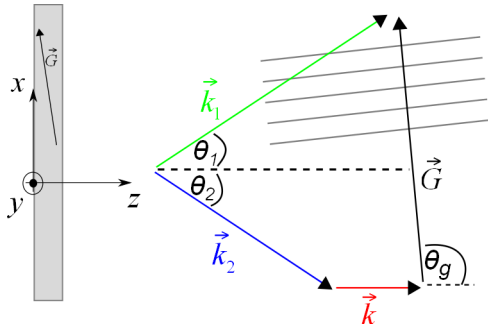

Fig. 1. Phase-matching diagram of DFG of optical radiation from two X-ray beams. k_1 and k_2 are the wave vectors of the pump pulses, k is the wavenumber of the optical beam, and G is the reciprocal lattice vector. θ_1, θ_2, and θ_g are the angles of the prorogation directions of the pumping beams, and the reciprocal lattice vector, respectively, with regard to the normal to the crystal surface. The solid lines represent the atomic planes of the crystal.

2.5 An example

We consider a specific example where the nonlinear medium is a diamond crystal and the reciprocal lattice vector normal to the (111) atomic planes is used for phase matching. The central photon energies of the pumping beams are 6.584 keV (λ = 1.8839 Å) and 6.582 keV (λ

#226995 - $15.00 USD Received 17 Nov 2014; revised 10 Feb 2015; accepted 12 Feb 2015; published 13 Mar 2015

= 1.8834 Å). The central photon-energy of the optical field, which is equal to the difference between the central frequencies of the pumping beams, is 1.9997 eV (λ = 620 nm). We assume that the pulse durations and waists of the two pumping beams are equal. The pulse duration τ is 50 fs and the waists in the $\hat{x}$ and $\hat{y}$ directions are 20 μm and 10 μm, respectively. The crystal length is 50 μm. To simplify the calculations, the angles of the pumping beams are chosen to have the same magnitude and opposite signs, namely $\theta_1 = -\theta_2 = \theta$, and the signal to be normal to the crystal surface ($\theta_s = 0$). The phase matching condition imposes an angle of θ_g between the reciprocal lattice vector and the normal of the crystal surface. The angles of the pumping beams and the reciprocal lattice vector with regard to the normal to the crystal surface are θ = 27.217° and θ_g = 90.029°, respectively [27]. The solution of Eq. (11) with $\Delta\tau_1 = 0$ can be written as

$$E(z) = \frac{i\sqrt{N}\,|\mathrm{Csc}\,\theta|}{16\pi k_z\sqrt{\frac{1}{w_x^2}+\frac{\tan^2\theta}{c^2\tau^2}}}\kappa\left[erf\left(\frac{iw_x\Delta\Omega\cot\theta}{2^{3/2}c}-\frac{\sqrt{2}z\sin\theta}{w_x}\right)-erf\left(\frac{iw_x\Delta\Omega\cot\theta}{2^{3/2}c}\right)\right] \tag{13}$$
$$\exp\left[-\frac{1}{8}\left(\tau^2\Delta\Omega^2+w_y^2\Delta k_y^2+\frac{\tau^2c^2w_x^2\Delta k_x^2}{c^2\tau^2\cos^2\theta+w_x^2\sin\theta}+\frac{w_x^2\Delta\Omega^2\cot^2\theta}{c^2}\right)\right]$$

here $\Delta\Omega$ is the deviation from the central optical frequency, Δk_x and Δk_y are the deviation from the central optical wave-number in the x-direction and y-direction, respectively. The error function in Eq. (13), which is defined as $erf(z) = \frac{2}{\sqrt{\pi}}\int_0^z \exp(-t^2)dt$, describes the overlap of the two pumping beams.

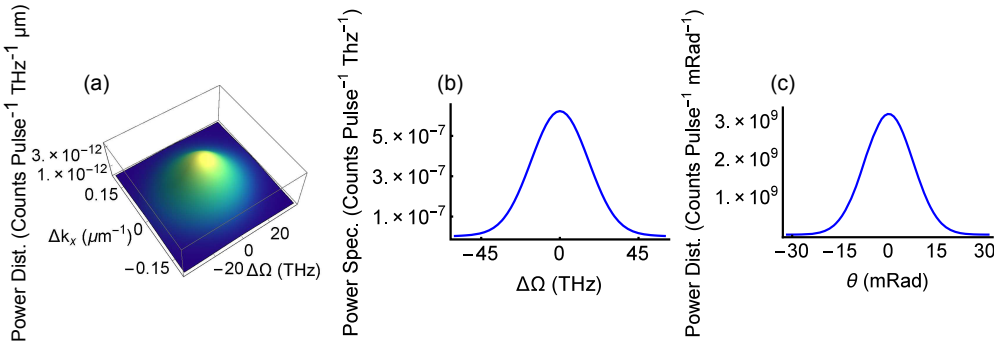

Fig. 2. Signal power distribution and spectra: (a) power distribution of the optical radiation as a function of deviation from the phase matching angle and the central frequency. (b) Power spectrum of the DFG signal. (c) Angular distribution of the DFG signal.

The power distribution of the optical signal as a function of frequency and the transverse wave-vector is shown in Fig. 2(a). The narrow frequency and the wave-vector (angular) bandwidths are determined by the phase matching bandwidth and are much narrower than the power distribution of the pump. In many experiments the power spectrum or the angular distribution of the power are measured. The power spectrum of the optical radiation is shown in Fig. 2(b). The power spectrum is obtained by integrating the power distribution over Δk_x. The full width at half maximum of the power spectrum is 38.68 THz (7.944 nm). This width can be resolved by using a conventional spectrometer. The angular distribution of the power is obtained by integrating the power distribution over the frequency. The result is shown in Fig. 2(c). The full width at half maximum of the angular distribution is 7.3 mrad, where refraction corrections are included.

#226995 - $15.00 USD Received 17 Nov 2014; revised 10 Feb 2015; accepted 12 Feb 2015; published 13 Mar 2015

Next, we examine the influence of the pulse duration, the beam size, and the crystal length on the power of the DFG process. The signal power is calculated by integrating over the frequency and angular range of the signal distribution as described in Fig. 2(a).

Since DFG is a nonlinear process, the intensity of the signal is expected to increase with shorter pulse durations and smaller spot areas of the X-ray beams, thus it is desirable to use short pulses and to focus the beams. However, as described earlier, the phase matching scheme imposes different propagation angles for the two pumping beams. Consequently, the temporal and spatial overlap distances between the X-ray beams can be shorter than the crystal length. Since the optical beam is generated only when the two pumping beams overlap, the overlap length is an important parameter for the description of the DFG process. As expected, our calculations indicate that the overlap length decreases with the reduction of the pulses durations and the beam sizes in the scattering plane. The dependence of the DFG power as a function of the pulse duration is described in Fig. 3(a). When the pulse duration of the pumping beams is very long, the pumping beams overlap, but the DFG power is weak since the peak intensity of the pumping beams is weak. As the pulse duration decreases, the peak intensity of pumping beams increases, but the overlap distance decreases. As long as the overlap distance is long enough, the increased peak intensities dominate and the DFG power increases with the reduction of the pulses duration, until the point where the influence of the reduction of the overlap is comparable to the influence of the enhancement of the peak intensity. At shorter pulses durations, the reduction of the overlap length dominates and the DFG power decreases with further reduction of the pulse duration. The dependence of the DFG power on the beam size in the scattering plane is very similar as shown in Fig. 3(b). When the pumping beams are broad, the dependence on the beam sizes is dominated by the peak intensity, and at small beam sizes, the short overlap distance reduces the DFG power. The beam size in the direction normal to the scattering plane does not affect the overlap. We find that the power of the optical signal increases with the crystal length (Fig. 3(c)) until the crystal length is longer than the overlap distance.

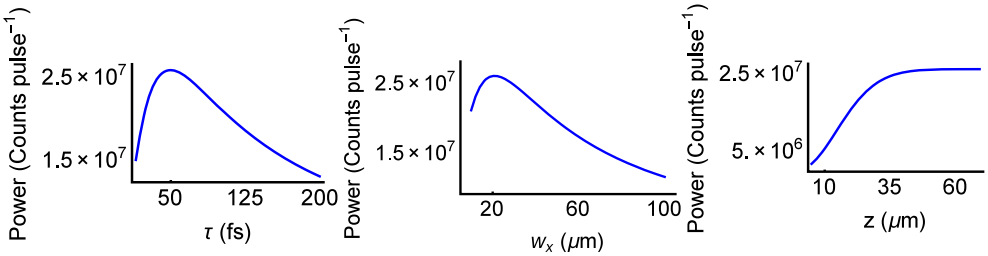

Fig. 3. Power of the optical radiation as a function of (a) pulse duration of the pump, (b) beam size of the pump, and (c) crystal length.

In the preceding paragraphs we analyzed the angular and the frequency dependencies of DFG from X-ray into optical wavelengths. These results are important for measurements with slow detectors, in particular with spectrometers. However, the use of ultrashort X-ray pulses suggests that DFG can be used for studies of processes occurring on short time scales. In this paragraph we describe the temporal properties of the process. The temporal shape of the optical signal is shown in Fig. 4(a). The typical pulse duration of the optical wave is a few hundred of femtoseconds. This time scale suggests that the use of fast detectors or time resolved spectroscopy techniques could improve the signal-to-noise ratio of the measurements. Nevertheless, the temporal resolution of the system is determined by the X-ray pulse duration. This is similar to autocorrelation techniques, which are widely used for the inspection of ultrashort optical pulses, where slow detectors are used, but the temporal resolution is determined by the short optical pulses. In Fig. 4(b) we plot the pulse-energy of the optical signal as a function of a delay between the X-ray pulses. This measurement constitutes a cross-correlation measurement. As expected, the comparison with the temporal shape of the pulse shown in Fig. 4(c) reveals that the cross-correlation of the two-pumping

#226995 - $15.00 USD Received 17 Nov 2014; revised 10 Feb 2015; accepted 12 Feb 2015; published 13 Mar 2015

beams corresponds to the pulse duration of the X-ray pulses. The small differences between the cross-correlation and the temporal shape of the pumping beams are introduced because the pumping beams are not collinear. We note that by decreasing (increasing) the pulse duration and the minimal waist size it is possible to decrease (increase) the duration of the cross-correlation signal.

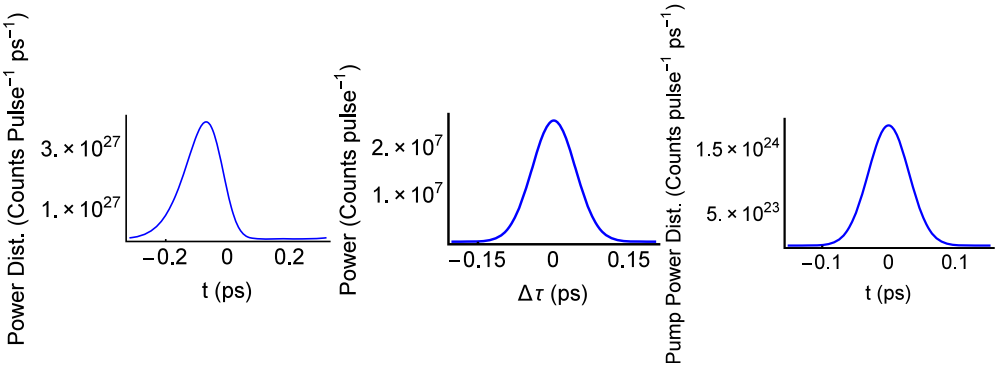

Fig. 4. (a) Temporal shape of the optical signal (b) Optical power as a function of delay between the two X-ray input beams (c) Pump power as a function of time.

3. Summery and discussion

In this work we analyzed the effect of DFG of optical waves from two-color X-ray pulses. We considered two transform-limited pump pulses and limited our discussion to pulse durations and beam sizes that allows the use of the slowly varying envelope approximation in order to give a clear representation of the main effects. We note that the present performances of XFELs are very close to our assumptions. Seeded nearly transform-limited [28] pulses at photon-energy of 6.6 keV, with about 10^{11} photons per pulse, and pulse durations of 50 fs (estimated) have been demonstrated at LCLS [29,30]. Our calculations show that the conversion efficiency can exceed 10^{-4}, which corresponds to count rates of more than 10^{7} optical photons per pulse. The wavelength and angular full width at half maximum bandwidth of the generated optical signal is a few milliradians and a few nanometers, respectively. The pulse duration is a few hundred of femtoseconds. We predict that the power spectrum can be resolved with conventional optical spectrometers [31].

For many materials the radiation damage threshold at X-ray wavelengths is many orders of magnitude larger than the damage threshold in the optical regime. For the specific case of synthetic diamonds we discus in this paper, the damage threshold at various wavelengths have been measured [32]. For example, the damage threshold at 532 nm is in the range of 0.8-1.1 GW/cm^2 and at 694 nm a damage threshold of 1.5 GW/cm^2 has been reported. The X-ray damage threshold is significantly higher. In a recent observation of X-ray second harmonic generation were the peak intensity of the pump was estimated to be 10^{16} W/cm^2, no radiation damages were observed [15]. Generally speaking, the radiation damage threshold at X-ray wavelengths scales with the photon-energies of the pumping beams. For light elements such as carbon, the photon energies of the X-ray beams are much larger than the biding energies of the electrons, thus effects such as cumulative ionization are expected to be negligible. For heavy elements, radiation damage at X-ray wavelengths is much smaller; hence the observation of DFG would require higher pump-energies.

A possible application of DFG of optical pulses from X-ray pulses is to probe the microscopic structure of valence electrons [1–3]. As is clearly shown in Eq. (12), the nonlinear current density, which drives the DFG process, is proportional to a Fourier component of the valence electrons, selected by phase matching. Therefore, the power of the DFG process is proportional to square of the absolute value of the unperturbed carrier density.

#226995 - $15.00 USD Received 17 Nov 2014; revised 10 Feb 2015; accepted 12 Feb 2015; published 13 Mar 2015

A series of measurements of the Fourier components of the valence electrons together with phase retrieval algorithm [33] can be used to reconstruct the valence electrons distribution.

Our work suggests that the DFG process we describe here would lead to higher efficiencies than sum/difference frequency mixing of X-ray and optical pumping beams. This is because the efficiency of the X-ray and optical mixing process depends on the intensity of the optical laser, thus limited by the optical damage threshold. On the other hand, the efficiency of the DFG process depends on the intensity of the X-ray lasers. Since the damage threshold at X-ray wavelengths is several orders of magnitude higher than the optical damage threshold, the intensity used for the pumping beams in DFG can be much higher than in X-ray and optical mixing. In addition, since the delay between the two pumping beams is controllable, it is possible to use DFG into optical wavelengths to probe the dynamics of processes, which are associated with valence electrons with temporal resolution determined by the duration of the X-ray pumping beams. With the present specifications of XFELs, the possible temporal resolution is a few of tens of femtoseconds. Another possible application is as a cross-correlator for the inspection of ultrashort X-ray pulses.

Acknowledgments

This work was supported by the Israel Science Foundation (under Grant No. 1038/13).

#226995 - $15.00 USD Received 17 Nov 2014; revised 10 Feb 2015; accepted 12 Feb 2015; published 13 Mar 2015